

# Measurement of Sr – N<sub>2</sub> elastic collision cross section in Magneto-Optical Trap

Chetan Vishwakarma,<sup>1</sup> Kushal Patel,<sup>1</sup> Jay Mangaonkar,<sup>1</sup> and Umakant D. Rapol<sup>1,2,\*</sup>

<sup>1</sup>*Department of Physics, Indian Institute of Science Education and Research, Pune 411008, Maharashtra, India*

<sup>2</sup>*Center for energy sciences, Indian Institute of Science Education and Research, Pune 411008, Maharashtra, India*

We experimentally measured the collision cross section between <sup>88</sup>Sr–N<sub>2</sub> and Sr–Sr in a Magneto Optical Trap (MOT). These collision cross sections are estimated by measuring the atomic loss rate as a function of background pressure of N<sub>2</sub> gas. The measurements performed here are important as N<sub>2</sub> is one of the prominent gases that remains in the vacuum chamber even after bake-out, directly affecting the trap lifetime. The knowledge of this cross section is imperative in order to quantify the contribution of background gas collisions in the total error budget of Strontium based optical atomic clock. We also estimate the loss rate caused by the combined effect of the decay of atoms in the long-lived <sup>3</sup>P<sub>0</sub> state and temperature induced atomic losses from the capture volume of the MOT. The later occurs due to a significant amount of time spent by the atoms in the states which are insensitive to the first stage cooling light. We find that the contribution of this channel is dominant in comparison to the other atomic loss channels. This experiment highlights the importance of including the temperature dependant loss channel in studies which rely on the measurement of total loss rate.

## I. INTRODUCTION

The invention of optical frequency comb [1] in conjunction with laser cooling techniques has boosted efforts towards using optical transitions as a universal time standard. Among various architectures [2], neutral atom based platforms have become popular in realizing the next generation optical clocks of which, Strontium (Sr) is one of the leading candidates. The Sr optical lattice clock [3] has been shown to offer a relative frequency uncertainty of  $2.5 \times 10^{-19}$  [4, 5]. With such precision and accuracy, it holds promise to revolutionize global time-keeping, measurement accuracy and stability of fundamental constants and precision sensing [2, 6, 7]. The total uncertainty budget of the clock transition is an addition of all the uncertainties caused by various factors e.g. AC Stark shift, Zeeman shift, black body radiation shift, background gas induced collisional shift etc. Systematic evaluation of the theses sources of uncertainties is one of the vital steps towards realizing the full potential of the clock transition. In this work, we report the measurement of collisional cross section, which is one of the limiting factors in improving the clock accuracy [8]. Collisions with background atomic/molecular species also limits the lifetime of the atomic sample. It is of utmost importance to quantify the effect of background gases on the atomic transition under consideration.

The collision cross section is traditionally determined using a crossed beam technique [9, 10]. In this method, two collimated atomic/molecular beams are produced and made to intersect in a well-defined interaction region. The determination of absolute collision cross section using this technique requires the knowledge of the exact number of target atoms and the volume of the intersection region of the beams. These are the two major sources of error in beam-based measurements. On

the other hand, measurements based on atomic loss rate from the MOT or a Magnetic Trap (MT) are shown to be more accurate in comparison to the earlier method [11]. In the same spirit, several theoretical and experimental works have been reported for the determination of collision cross-section between various atomic species [12–14]. As the loss rate of atoms depends on the trap-depth, such methods can also be employed for the determination of the degree of confinement of the trapping potentials [15, 16].

In this article, we report the first experimental determination of Sr–N<sub>2</sub> by measuring the loss rate of atoms from <sup>88</sup>Sr blue MOT. We consider the various loss mechanisms in MOT and evaluate their contributions. These additional contributions have been used to measure the Sr–Sr collision cross section. In our experiment, the total atomic loss rate depends on (i) the collision with untrapped background atoms/molecules, (ii) the decay of atoms into the long-lived triplet state <sup>3</sup>P<sub>0</sub> and (iii) the temperature of the atomic cloud. In our experiment, <sup>3</sup>P<sub>0</sub> state is connected to the first stage cooling via <sup>1</sup>D<sub>2</sub> and the repumping transition at 707 nm. The atoms in state <sup>3</sup>P<sub>0</sub> take a relatively longer time to return to the primary cooling cycle and thus contribute to the atom loss rate. We show that escape of atoms from the trapping region due to the branching into states which are unresponsive to the cooling laser beams can significantly contribute towards atomic loss rate. This loss channel is proportional to the atomic cloud temperature and is the dominant loss channel for the atomic species which require two stages of cooling. The contribution of this term along with losses induced by decay into the long-lived state is determined by studying the loss rate as a function of the intensity of the MOT beams.

\* Electronic mail: [umakant.rapol@iiserpune.ac.in](mailto:umakant.rapol@iiserpune.ac.in)

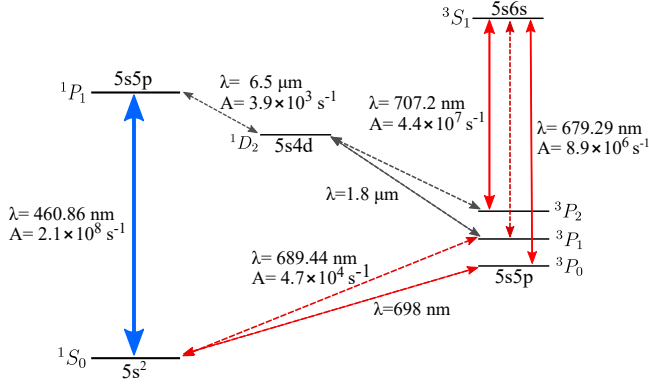


FIG. 1. The relevant low-lying energy level diagram of Strontium ( $^{88}\text{Sr}$ ) atoms. The wavelength ( $\lambda$ ) and the decay rate ( $A$ ) has been shown along the transition.

## II. THEORETICAL BACKGROUND

The experiment is performed with the most abundant even isotope of Strontium ( $^{88}\text{Sr}$ ). Fig.1, shows the low lying energy level diagram of Sr atom. It has two possible cooling transitions  $5s^2 \ ^1S_0 \rightarrow 5s \ 5p \ ^1P_1$  and  $5s^2 \ ^1S_0 \rightarrow 5s \ 5p \ ^3P_1$  of wavelengths 460.8 nm and 689.4 nm respectively. The doubly forbidden singlet to triplet transition ( $^1S_0 \rightarrow ^3P_1$ ) has a long lifetime of 21  $\mu\text{s}$  and linewidth of  $2\pi \times 7.5 \text{ kHz}$ . This transition can be used for the second stage of cooling and has extremely low Doppler limited temperature of  $\sim 180 \text{ nK}$ . The other cooling transition connects  $^1S_0 \rightarrow ^1P_1$ . This transition has a very short lifetime of  $\sim 5 \text{ ns}$  ( $\Gamma = 2\pi \times 32 \text{ MHz}$ ) and is well suited for the first stage of cooling and trapping. However, it has a disadvantage of higher Doppler limited temperature of  $\sim 770 \mu\text{K}$ ; further, the transition itself is not completely closed. The atoms when excited to  $^1P_1$  state, decays to  $^1D_2$  state with a branching ratio of  $1:2 \times 10^{-5}$ . Atoms in  $^1D_2$  further decay to  $^3P_2$  and  $^3P_1$  states with a branching ratio of  $1:2$  respectively. The transition  $^3P_2 \rightarrow ^1S_0$  state is forbidden, and hence the atoms once decayed to  $^3P_2$  are lost from the cooling cycle. There are several repumping schemes to minimize this loss [17]. The most popular of them employs two lasers operating at 707.2 nm and 679.3 nm. The decay rates and wavelengths of the relevant transitions are shown in Fig.1 along with the possible repumping scheme.

The collision between a background particle (atoms/molecules) and a trapped atom is often considered as an elastic process. At room temperature, the untrapped background particles have sufficient energy to knock the atoms out of the trap. This collisional process can limit the lifetime of atoms in the trap and is directly proportional to the background pressure in the vacuum chamber. The loading of atoms in the MOT is a dynamic process, and a steady-state population is achieved on attaining equilibrium between the loading and the loss rate. The rate equation can be written as:

$$\frac{dN}{dt} = R - \frac{N}{\tau} - \beta N^2 \quad (1)$$

In the above expression,  $N$  is the number of atoms at a given instant of time,  $R$  is the loading rate,  $1/\tau$  is the linear loss rate of atoms, and  $\beta$  represents the non-linear loss rate due to intra-trap collisions. The experiments reported in this article have been performed in the linear regime, and thus the term which is quadratic in  $N$  is neglected [18] for further analysis. In the low-density regime, the solution of Eq.1 displays an exponential growth in the number of atoms in MOT and can be written as  $N = N_s [1 - \exp(-\frac{t}{\tau})]$ , where,  $N_s = R\tau$ .

The linear loss rate in Eq.1 can be attributed due to several factors, viz, (a) collision with residual background atoms, (b) collision with untrapped Sr atoms, (c) decay into the metastable states and (d) escape of atoms out of the capture region. By combining the factors mentioned above, the total linear loss rate can be written as:

$$\frac{1}{\tau} = n_b \sigma_b v_b + n_{Sr} \sigma_{Sr} v_{Sr} + \alpha_x f + \epsilon \gamma t \frac{A \ ^1P_1 \rightarrow \ ^1D_2 \ f}{A \ ^1D_2 \rightarrow \ ^3P_2 + A \ ^1D_2 \rightarrow \ ^3P_1} \quad (2)$$

Here,  $n$  is the density of the background particle,  $\sigma$  is the classical collision cross-section, and  $v$  is the average velocity of the particle under consideration. The subscript  $b$  and  $Sr$  denotes background atoms and Strontium respectively. The third term ( $\alpha_x f$ ) in the above equation denotes the loss of atoms due to branching into the metastable state  $x$ . In our experiment (considering cooling and repumping lasers at 460.8 nm and 707.2 nm respectively), such a loss corresponds to the effective decay of atoms into the long-lived state  $^3P_0$  and is denoted by  $\alpha_0 f$ . The atoms in excited state  $^1P_1$  decay to the intermediate state  $^1D_2$  with the rate  $A \ ^1P_1 \rightarrow \ ^1D_2$ . These atoms can further decay to  $^3P_2$  state with the branching ratio  $B \ ^1D_2 \rightarrow \ ^3P_2$ . A fraction of atoms is excited into the  $^3S_1$  state with the repumping laser ( $\lambda = 707.2 \text{ nm}$ ). These atoms can make a transition from  $^3S_1$  to  $^3P_0$  state with the branching ratio  $B \ ^3S_1 \rightarrow \ ^3P_0$ . This state is weakly coupled to the ground state  $^1S_0$  and has a relatively long lifetime. Thus, populating the  $^3P_0$  state is considered as the loss channel. This loss rate can be written as [19]:

$$\frac{1}{\tau_{power}} = \alpha_0 f = (f A \ ^1P_1 \rightarrow \ ^1D_2) (B \ ^1D_2 \rightarrow \ ^3P_2) (f' B \ ^3S_1 \rightarrow \ ^3P_0) \quad (3)$$

Here,  $f$  and  $f'$  is the fraction of atoms in the excited state  $^1P_1$  and  $^3S_1$  respectively. This fraction can be given as:

$$f = \frac{1}{2} \frac{I/I_0}{1 + I/I_0 + (2\Delta/\Gamma)^2} \quad (4)$$

where,  $I$  is the total intensity,  $I_0$  is the saturation intensity of the transition,  $\Delta$  is detuning of the laser beam, and  $\Gamma$  is natural line-width of the transition under consideration.

The last term  $\left(\tau_{temp}^{-1} = \epsilon\gamma_t \frac{A_{1P_1 \rightarrow 1D_2} f}{A_{1D_2 \rightarrow 3P_2} + A_{1D_2 \rightarrow 3P_1}}\right)$  in Eq.2 denotes the atomic loss due to escape from the capture region [20]. The term  $A_{1D_2 \rightarrow 3P_2}$  denotes the decay rate from the intermediate state  $1D_2$  to the triplet state  $3P_2$ . This loss channel can be understood as follows. A fraction of atoms from the excited state  $1P_1$  decay to the intermediate state  $1D_2$ , which further connects to two triplet states  $3P_2$  and  $3P_1$  as shown in Fig.1. The atoms in  $3P_1$  state decay to the ground state in 21  $\mu$ s. On the other hand, the atoms which have decayed to  $3P_2$  state can be brought back to the main cooling transition by using a repumper at 707.2 nm. However, in the absence of repumping laser of wavelength 679.3 nm, the atoms are accumulated into the atomic state  $3P_0$ . Considering all the cascaded channels, it takes  $\sim 1$  ms ( $\equiv \gamma_t^{-1}$ ) for the atoms in  $1D_2$  to return to the ground state via  $3P_2$  and  $3P_1$  state. During this process, the atoms are not responsive to the main cooling laser operating at 460.8 nm and therefore have a finite probability of escaping from the capture region of MOT. Such probability is determined by the diameter of the MOT beams and the average temperature of the atomic ensemble. The probability ( $\epsilon$ ) for the atoms to escape the trapping region of MOT is given by [20]:

$$\epsilon \sim \int_0^\infty \left(\frac{1}{2\pi v_0^2}\right)^{\frac{3}{2}} 4\pi v^2 \exp\left(\frac{-v^2}{2v_0^2}\right) \exp\left(\frac{-R\gamma_t}{v}\right) dv \quad (5)$$

Here,  $v_0$  and  $R$  denotes the root mean square velocity of the atoms and the radius of the trapping beam respectively.

After identification of various loss mechanisms, the individual contributions have been evaluated by operating the MOT at different experimental conditions. The measurement of the total loss rate as a function of power in the trapping beams and density of the background gas provides relevant information regarding the collision cross-section and losses because of branching into the long-lived state. The temperature of the atomic cloud is measured to take into account the atomic losses due to the thermal motion.

### III. EXPERIMENTAL DETAILS

The experiments are performed using the blue MOT of  $^{88}\text{Sr}$  atoms formed inside a cuboidal quartz cell having dimensions of 38 mm  $\times$  38 mm  $\times$  160 mm. We use an effusive source [21] of atoms which is resistively heated to 600°C. These atoms are then slowed down by a zero-crossing Zeeman slower in order to load the MOT. The MOT laser beams are prepared following the standard  $\sigma^+ - \sigma^-$  configuration with retro-reflection geometry. Each laser

beams have  $1/e^2$  diameter of 10 mm and maximum intensity of  $\sim 20$  mW/cm<sup>2</sup>. The light for the laser cooling in blue MOT ( $5s^2 1S_0 \rightarrow 5s 5p 1P_1$ ,  $I_s = 42.7$  mW/cm<sup>2</sup>) is generated using a homemade cavity-enhanced optical frequency doubler. The frequency doubler uses a periodically poled KTP crystal for Second Harmonic Generation (SHG). This cavity is injected with an input laser ( $\lambda = 922$  nm, power = 700 mW) light from a commercial tapered amplifier. The seed light for the amplifier is generated using a grating-stabilized diode laser in Littrow configuration. The frequency of the laser is stabilized to the cooling transition by performing atomic beam spectroscopy [22]. The magnetic field for the MOT is generated using a pair of anti-Helmholtz coils which produces an axial field gradient of  $\sim 44$  Gauss/cm. During the loading of atoms in MOT, detuning of the MOT laser beams are kept at  $-33$  MHz. The decay of atoms into the metastable state  $3P_2$  is suppressed using a repumping laser of wavelength 707.2 nm operating at the atomic transition  $5s 5p 3P_2 \rightarrow 5s 6s 3S_1$  ( $I_s = 3.4$  mW/cm<sup>2</sup>) as shown in Fig.1. The frequency of the repumping laser is locked using a digital PID controller which receives the feedback of the laser frequency via a commercial wavemeter (High Finesse, WSU-30).

The number of trapped atoms in MOT is estimated by collecting the fluorescence of the atoms on a calibrated photomultiplier tube (Hamamatsu-H9307-02). Typical loading curves with two different trapping intensities are shown in Fig.2. We load  $\sim 10^6$  number of atoms in MOT within  $\sim 400$  ms.

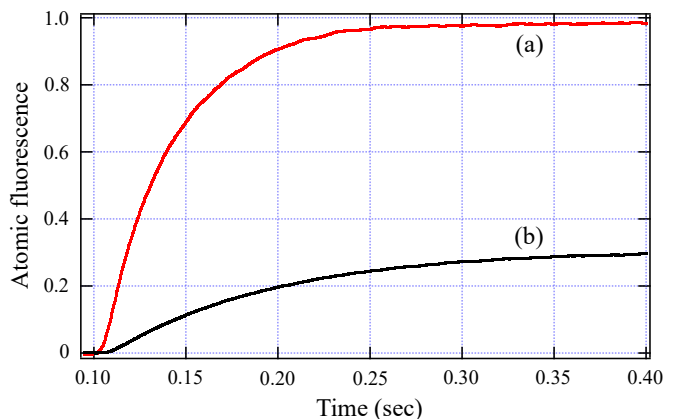


FIG. 2. Normalized fluorescence of  $^{88}\text{Sr}$  MOT for two different trapping intensities, (a) total intensity 96.8 mW/cm<sup>2</sup> and (b) 31 mW/cm<sup>2</sup>. All the remaining parameters are kept constant.

The determination of the collision cross-section is based on the change in the MOT loading rate on the introduction of gas species inside the vacuum chamber. The vacuum system for the current experiment consists of mainly two sections – the oven region and the quartz cell connected to the Zeeman slower tube. These two regions are separated by a differential pumping tube. The pressure in these sections is maintained by two indepen-

dent ion pumps (capacity  $\sim 55 \text{ l s}^{-1}$ ) connected to both the regions. Also, a Titanium Sublimation Pump (TSP) is connected to the science chamber (near the quartz cell) for maintaining the desired low pressure. The base pressure inside the quartz cell is less than  $1 \times 10^{-10}$  torr. In the current experiment, the MOT loading curves at different background pressures are used to determine the collision cross section between the species of our interest. A leak valve is connected to the quartz cell via an all-metal right angle valve for releasing the background species in a controlled manner. The other end of the leak valve is connected to a gas cylinder containing high purity (99.999%)  $\text{N}_2$  gas which is used as the background species in our experiment. Since the vacuum pumps connected to the system continuously pump out the background gas, specific leak rates of  $\text{N}_2$  gas is used to achieve desired values of equilibrium pressure of  $\text{N}_2$  in the chamber. The loading of atoms in the MOT is recorded using a PMT at different equilibrium pressure levels.

In order to study the dependence of the loss rate on the power of the trapping laser beams, the MOT is operated at different powers while keeping all other experimental parameters unchanged. The losses of atoms induced by the thermal motion are characterized by measuring the temperature of the atomic cloud. We use the *release and recapture* technique [23] to determine the average temperature of the atomic cloud. In this experiment, the release time has been varied from 1 ms to 30 ms, and the fluorescence of the recaptured atoms is recorded.

#### IV. RESULTS AND DISCUSSION

In order to measure the  $^{88}\text{Sr}-\text{N}_2$  and Sr–Sr collision cross-section, we have used the formulation represented in Eq.2. The validity of Eq.2 demands the MOT to be operated in the low-density regime which is manifested by the exponential growth of the number of atoms in MOT [12, 18, 24]. Fig.2 displays two clear exponential profiles of the MOT loading curves recorded at two extreme operating powers (a.  $96.8 \text{ mW/cm}^2$  and b.  $31 \text{ mW/cm}^2$ ) of the trapping laser beams.

We have carried out experiments at different background pressures to evaluate the  $^{88}\text{Sr}-\text{N}_2$  collision cross-section. Fig.3 represents the total loss rate of atoms as a function of the density of  $\text{N}_2$  molecules. Considering the loss rate for two different background pressures, Eq.2 can be modified as:

$$\frac{1}{\tau_h} - \frac{1}{\tau_l} = \{n_b^h - n_b^l\} \sigma_b v_b \quad (6)$$

Here, the superscript  $h$  and  $l$  denotes the two different cases of high and low background pressures respectively. On increasing the pressure of  $\text{N}_2$ , the total loss rate exhibits a linear increase with a slope of  $\sigma_b v_b$  (as predicted in Eq.6). The knowledge of the values of the background densities ( $n_b^h$  and  $n_b^l$ ) and the average velocity ( $v_b$ ) of  $\text{N}_2$

atoms at room temperature enables us to calculate the value of  $^{88}\text{Sr}-\text{N}_2$  collision cross-section. Since  $\text{N}_2$  atoms are in thermal equilibrium with the vacuum system, we have used  $v_b = 470 \text{ ms}^{-1}$  as calculated at room temperature ( $20^\circ\text{C}$ ). We found the average value of  $^{88}\text{Sr}-\text{N}_2$  collision cross section to be  $\sigma_b = 8.1(6) \times 10^{-18} \text{ m}^2$  which is comparable to a similar experimental result performed with Rb and Na using the same background species ( $\text{N}_2$ ) Ref.[14].

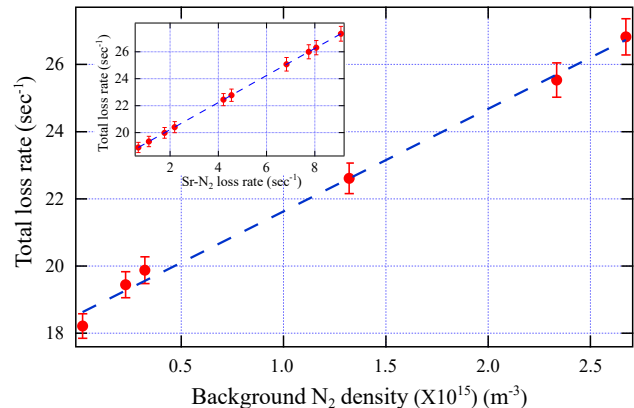


FIG. 3. Loss rate of atoms in Sr MOT as a function of background  $\text{N}_2$  density. Inset: The total loss rate as a function Sr– $\text{N}_2$  loss rate. It shows that the contribution due to other loss channels such as power dependent loss and loss due to cloud temperature remains constant for constant trapping power.

Using Eq.2 for the calculation of Sr–Sr collision cross section requires the knowledge of the loss rate due to (a) background  $\text{N}_2$  molecules, (b) decay of atoms into long-lived triplet state  $^3P_0$  and (c) escape of atoms from the trapping region. We proceed with the estimation of  $\tau_{power}^{-1}$  and  $\tau_{temp}^{-1}$  of Eq.2 as mentioned in the earlier section. Power dependent losses, represented by  $\tau_{power}^{-1}$ , occurs due to the decay of atoms from the excited state ( $^1P_1$ ) to the metastable state  $^3P_2$ . However, the presence of repumping laser at  $707.2 \text{ nm}$ , brings these atoms back to the triplet states via excited state  $^3S_1$ . The branching ratio for  $^3P_2$ ,  $^3P_1$  and  $^3P_0$  are  $5/9$ ,  $3/9$  and  $1/9$  respectively [25]. In the absence of  $679.3 \text{ nm}$  repumping light, the atoms eventually decay into the state  $^3P_0$  and go out of the cooling cycle. On the other hand, temperature dependent loss denoted by the fourth term in Eq.2, occurs due to the transfer of atoms into states which are insensitive to the laser used for the first stage of cooling. Since the atoms in these states do not experience any force, they are free to go out of the MOT capture region. The decay probability to such states is proportional to the fraction of atoms in the excited state  $^1P_1$ .

Since, the terms mentioned above are functions of the fraction of atoms in the excited state, during the experiment we can not determine the individual contributions but only observe the combined effect.

In order to determine the combined contribution of



power and temperature dependent losses, the MOT is operated at different intensities of trapping laser beams. For analysis, we have assumed that  $\sigma_b$  and  $\sigma_{Sr}$  are independent of the power of laser beams ( $\lambda = 460.8$  nm). Assuming that the probability of atoms to escape the capture region of MOT is independent of the trapping beam power, the following relationship can be written using Eq.2:

$$\frac{1}{\tau_1} - \frac{1}{\tau_2} = \{f_1 - f_2\}\alpha \quad (7)$$

Here, the subscripts 1, 2 denotes the MOT loading at two different powers, and  $\alpha$  is the proportionality constant for the combined losses of atoms due to decay into  $^3P_0$  and due to escape from the trapping region. Thus,  $\alpha$  can be written as:

$$\alpha = \alpha_0 + \epsilon\gamma_t \frac{A_{^1P_1 \rightarrow ^1D_2}}{A_{^1D_2 \rightarrow ^3P_2} + A_{^1D_2 \rightarrow ^3P_1}} \quad (8)$$

In order to check the validity of Eq.7, we have carried out an experiment for the measurement of the temperature of the atomic cloud with different intensities of MOT beams. The variation was found to be  $\sim 0.3$  mK, which is within the error of our experimental data. This allows us to use Eq.7 for the calculation of power and temperature dependent loss rate. The value of  $\alpha$  is extracted by fitting,  $1/\tau = \alpha f + c$  to the plot of total loss rate as a function of intensities of MOT beams as shown in Fig.4. In the above equation, the intercept  $c$  on the vertical axis and signifies the loss rate limited solely by the quality of vacuum inside the science chamber. The fitting gives the value of  $\alpha = 167(4) \text{ s}^{-1}$ . The intercept of this curve is  $1.2(4) \text{ s}^{-1}$ . To get the individual contributions, we theoretically calculate the value of  $\tau_{power}^{-1}$  using Eq.3. Appropriate quantities for the calculation have been taken from Fig.1. The calculation yields a relatively small value of  $\alpha_0 \sim 33 \text{ s}^{-1}$ . The contribution due to temperature dependent loss channel is obtained by subtracting the value of  $\alpha_0$  from  $\alpha$  and is found to be  $134(4) \text{ s}^{-1}$ .

Experimental determination of thermal loss channel requires the knowledge of escape probability of the atoms from the capture region which is proportional to the temperature of the atomic cloud. Temperature is measured using the standard *release and recapture* technique. In this technique, the fraction of atoms recaptured in the trap is measured as a function of release time. This recaptured fraction is inversely proportional to the rate of expansion of the atomic cloud and is used for the determination of temperature. In our experiment, we get an average temperature of  $3.6(3)$  mK. Eq.5 is used for the calculation of  $\epsilon$  and the value is found to be  $\sim 0.06$ . This value is used to calculate  $\tau_{temp}^{-1}/f$  and the resulting loss rate is found to be  $120(15) \text{ s}^{-1}$ . Incorporating the temperature dependent losses with the calculated power dependent losses ( $\alpha_0$ ), we get  $\alpha = 153(15) \text{ s}^{-1}$ , which

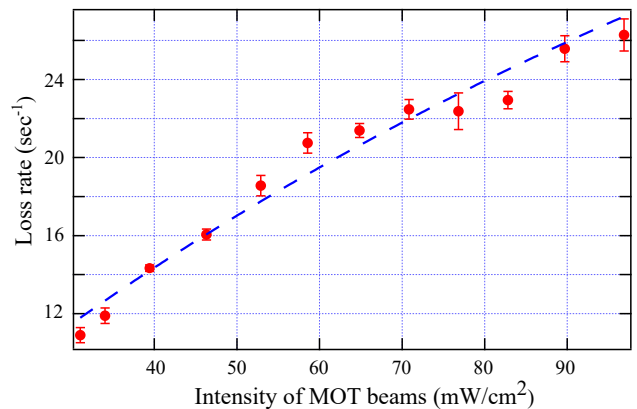


FIG. 4. Loss rate of atoms in Sr MOT as a function of trapping beam intensity. The data is taken in presence of single repumping laser. The detuning and axial field gradient for the MOT is kept at  $-33$  MHz and  $48$  gauss/cm respectively.

agrees with the experimental measurement ( $\alpha = 167 \text{ s}^{-1}$ ) within error.

The experimentally determined value of  $\sigma_b$  and  $\alpha$  are used for the calculation of Sr–Sr collision cross section with the help of Eq.2. The calculation requires the knowledge of average velocity and the density of background Sr atoms. For the purpose of calculation, it is assumed that the background Sr atoms are in thermal equilibrium with the vacuum chamber and hence follows the Maxwell-Boltzmann distribution at room temperature. The density and average velocity of background Sr atoms are taken to be constant at  $3.2 \times 10^{12} \text{ m}^{-3}$  and  $265 \text{ ms}^{-1}$  respectively. The calculated value of Sr–Sr collision cross section is found to be  $6.0(9) \times 10^{-15} \text{ m}^2$ . The difference between  $^{88}\text{Sr}-\text{N}_2$  loss rate and the total loss rate is a constant for various background pressures as predicted by Eq.2. It signifies that the linear increase in total loss rate with the increase in pressure is solely due to  $^{88}\text{Sr}-\text{N}_2$  collision channel and not because of  $\tau_{power}^{-1}$ ,  $\tau_{temp}^{-1}$  or Sr–Sr collision induced loss. This linearity is shown in the inset of Fig.3. This statement is valid only for constant power of MOT beams.

## V. CONCLUSION

In conclusion, we have studied the loss rate of  $^{88}\text{Sr}$  atoms in blue MOT in the presence of a single repumping laser operating at  $707$  nm. The effect of background  $\text{N}_2$  molecules on the total loss rate is studied and is used for the determination of collision cross sections between  $^{88}\text{Sr}-\text{N}_2$  and its value is found to be  $8.1(6) \times 10^{-18} \text{ m}^2$ . We characterize the various loss channels and determine their contributions towards the total loss rate. We show that the dominant loss channel is from the combined effect of time taken by the atoms to return to the primary cooling cycle via the intermediate states and the thermal escape of atoms from the trapping region during this pe-

riod. The other contributing loss channel is the decay of atom into the long-lived state  $^3P_0$ . For the current experimental setup, their collective contribution ( $\alpha$ ) is estimated by operating the MOT at different intensities of trapping beams. The combined decay rate is found to be  $167(4) s^{-1}$ . The experimentally determined value of  $\alpha$  and  $\sigma_b$  have been used for the calculation of collision cross section between Sr–Sr. The calculated value of collision cross section for Sr–Sr collisions measured to be  $6.0(9) \times 10^{-15} m^2$ .

## VI. ACKNOWLEDGEMENT

The authors would like to thank the Department of Science and Technology, Govt. of India for grants through EMR/2014/000365. The authors are grateful to IISER Pune for providing funds and a great working environment.

- 
- [1] S. T. Cundiff and J. Ye, *Rev. Mod. Phys.* **75**, 325 (2003).  
 [2] A. D. Ludlow, M. M. Boyd, J. Ye, E. Peik and P. O. Schmidt, *Rev. Mod. Phys.* **87**, 637 (2015)  
 [3] A. Derevianko and H. Katori, *Rev. Mod. Phys.* **83**, 331 (2011).  
 [4] T. Nicholson, S. Campbell, R. Hutson, *et al.*, *Nature Commun.* **6**, 6896 (2015).  
 [5] G. E. Marti, R. B. Hutson, A. Goban, S. L. Campbell and N. Poli, J. Ye, *Phys. Rev. Lett.* **120**, 103201 (2018).  
 [6] G. Tino, L. Cacciapuoti, K. Bongs, *et al.*, *Nuclear Physics B - Proceedings Supplements* **166**, 159 (2007), Proceedings of the Third International Conference on Particle and Fundamental Physics in Space.  
 [7] S. N. Lea, *Reports on Progress in Physics* **70**, 1473 (2007).  
 [8] N. Shiga, Y. Li, H. Ito, S. Nagano, *et al.*, *Phys. Rev. A* **80**, 030501 (2009).  
 [9] D. Rickey and J. Krenos, *The Journal of Chemical Physics* **106**, 3135 (1997).  
 [10] R. Kau, I. D. Petrov, V. L. Sukhorukov and H. Hotop, *Journal of Physics B: Atomic, Molecular and Optical Physics* **29**, 5673 (1996).  
 [11] K. J. Matherson, R. D. Glover, D. E. Laban and R. T. Sang, *Phys. Rev. A* **78**, 042712 (2008).  
 [12] U. D. Rapol, A. Krishna, A. Wasan and V. Natarajan, *The European Physical Journal D - Atomic, Molecular, Optical and Plasma Physics* **29**, 409 (2004).  
 [13] K. J. Matherson, R. D. Glover, D. E. Laban and R. T. Sang, *Rev. Sci. Instrum.* **78**, 073102 (2007).  
 [14] U. D. Rapol, A. Wasan and V. Natarajan, *Phys. Rev. A* **64**, 023402 (2001).  
 [15] M. Haw, N. Evetts, W. Gunton, J. V. Dongen, J. L. Booth and K. W. Madison, *J. Opt. Soc. Am. B* **29**, 475 (2012).  
 [16] J. Van Dongen, C. Zhu, D. Clement, G. Dufour, J. L. Booth and K. W. Madison, *Phys. Rev. A* **84**, 022708 (2011).  
 [17] S. Stellmer and F. Schreck, *Phys. Rev. A* **90**, 022512 (2014).  
 [18] T. P. Dinneen, K. R. Vogel, E. Arimondo, J. L. Hall and A. Gallagher, *Phys. Rev. A* **59**, 1216 (1999).  
 [19] X. Xu, T. H. Loftus, J. L. Hall, A. Gallagher and J. Ye, *J. Opt. Soc. Am. B* **20**, 968 (2003).  
 [20] T. Kurosu and F. Shimizu, *Jpn. J. Appl. Phys.* **31**, 908 (1992).  
 [21] C. Vishwakarma, J. Mangaonkar, K. Patel, G. Verma, S. Sarkar and U. D. Rapol, arXiv preprint, arXiv:1810.09090 (2018).  
 [22] G. Verma, C. Vishwakarma, C. V. Dharmadhikari and U. D. Rapol, *Rev. Sci. Instrum.* **88**, 033103 (2017).  
 [23] L. Russell, R. Kumar, V. Tiwari and S. N. Chormaic, *Opt. Commun.* **309**, 313 (2013).  
 [24] T. Loftus, J. R. Bochinski, R. Shivitz, T. W. Mossberg, *Phys. Rev. A* **61**, 051401 (2000).  
 [25] T. Ido and H. Katori, *Phys. Rev. Lett.* **91**, 053001 (2003).